

# Severe Plastic Deformation of Steels

S. Scheriau, and R. Pippan

In order to demonstrate the structural changes in steels during severe plastic deformation (SPD), Armco iron, a ferritic steel P800 and a pearlitic rail steel S900A are subjected to a high pressure torsion (HPT) deformation process. The microstructural evolution, the changes in microhardness and the flow stress behaviour are investigated. Depending on the main process parameters like the deformation temperature and the applied strain, the impact of alloying on the evolving microstructure is studied in detail. The results clearly show that pure metals and single phase alloys follow a relatively uniform deformation behaviour. With increasing strain the structural size decreases ending in saturation at an equivalent strain between 10 and 30. In the case of the pearlitic rail steel a continuous growth in shear stress without saturation is investigated in the range of the applied strains. The microstructures of the examined materials Armco iron and P800 contain an ultra fine grain structure whereas for alloy S900A the initially randomly oriented lamellae are heavily bent and broken into small fragments. Possible reasons for the observed differences in the deformation behaviour are discussed.

*Hochverformung von Stählen.* Armco Eisen, ein ferritischer Stahl P800 und ein perlitischer Schienenstahl S900A wurden über den Prozess der Hochdruck-Torsion verformt. Untersucht werden die Entwicklung der Mikrostruktur, die Veränderungen in der Mikrohärtigkeit und das Fließspannungsverhalten. Neben den bestimmenden Verformungsparametern wie Umformtemperatur und aufgebrachte Dehnung wird der Legierungseinfluss auf die Mikrostruktur der umgeformten Metalle genauer erforscht. Die Ergebnisse für Reinmetalle und einphasige Legierungen haben gezeigt, dass mit zunehmender Dehnung die Strukturgröße sinkt und bei einer Vergleichsdehnung zwischen 10 und 30 die Sättigung erreicht wird. Für den Schienenstahl wurde bei den aufgebrachten Dehnungen keine Sättigung beobachtet. Das Torsionsmoment nimmt mit steigender Dehnung zu. Die Mikrostruktur der untersuchten Materialien Armco Eisen und P800 beinhaltet sehr feine, im Bereich zwischen 50 und 500 nm große Körner. In der Verformungsstruktur des S900A erkennt man deutlich, dass die anfangs zufällig orientierten Perlitlamellen mit zunehmender Dehnung verbogen werden, ehe sie in kleinere Fragmente zerbrechen und sich parallel zur Scherrichtung anordnen.

## 1. Introduction

Over the last 15 years, the interest in research on processing, microstructure evolution and mechanical behaviour of ultrafine grained ( $d < 1 \mu\text{m}$ ) and nanocrystalline ( $d < 100 \text{nm}$ ) materials have grown enormously. These materials became available in large quantities with the development of new effective techniques of severe plastic deformation (SPD), such as equal channel angular pressing (ECAP), accumulative roll-bonding (ARB), cyclic extrusion compression (CEC) and high pressure torsion (HPT)<sup>1-4</sup>. All the aforementioned techniques have in common that a coarse grained, bulk solid material is taken and processed through heavy straining into an ultrafined or even nanosized microstructure<sup>5</sup>.

It is well known that plastic deformation to very large strains below recrystallization temperature results in a structural refinement. In this case the dislocations are not randomly distributed; they form a cellular substructure with low misorientations between the cells. In con-

trast, the microstructures formed by SPD consist of small grains mainly divided by high angle boundaries. The resulting unique physical and mechanical properties like very high strength and often good ductility are based on the dense (non porous) bulk character of the processed materials<sup>6,7</sup>.

Most studies are focused on aluminium, copper, titanium and nickel alloys; steels are not frequently investigated. The aim of the present paper is to study the influence of the main deformation parameters of HPT on the evolving microstructures of different iron based alloys. The severe plastic shear deformation behaviour of two steels and pure iron is investigated in order to understand the processes during heavy deformation up to the steady state of microstructural refinement.

## 2. Experimental

### 2.1 Materials and Materials Processing

The materials investigated are Armco iron, a ferritic steel P800 and a coarse-pearlitic steel S900A. The ferritic and the pearlitic steels were provided by Böhler Edelstahl GmbH and Voestalpine Schienen GmbH, respectively.

---

*Dipl.-Ing. Stephan Scheriau*, Erich Schmid Institute of Materials Science, Austrian Academy of Sciences, Jahnstraße 12, 8700 Leoben / Austria; *Univ.-Prof. Dipl.-Ing. Dr. mont. Reinhard Pippan*, Christian Doppler Laboratory for Local Analysis of Deformation and Fracture, Jahnstraße 12, 8700 Leoben / Austria.

Table 1: Chemical composition of impurities (mass %) in the investigated materials; the balance is Fe

	C	Si	Mn	Cr	Ni	Co	P	S
Armco Fe	0.007	0.007	0.08	0.02	0.03	–	0.11	–
P800	0.03	1.3	1.2	1.4	0.15	17	–	–
S900A	0.76	0.35	1	0.014	–	–	0.017	0.04

The chemical composition of the materials is given in Table 1.

An annealing for 1 h at 873 K was performed on the base material, Armco iron, in order to remove existing deformation pattern. The resulting mean grain size was approximately 40  $\mu\text{m}$ . In the case of the ferritic steel the initial grain size was about 22  $\mu\text{m}$  and the size of the pearlite colonies in the rail steel was in the range of 10 to 20  $\mu\text{m}$ . To investigate the evolving deformation structures during SPD, the coin-like samples with the typical dimensions of 8 mm in diameter and 0.8 mm in thickness were subjected to high pressure torsion. All samples were deformed at a hydrostatic pressure of 6 GPa. The number of rotations was selected to obtain equivalent strains  $\epsilon$  of 4, 8, 16, 32 at a radius of 3 mm. The strain is well defined as simple shear,  $\gamma$ , and is calculated according to the equation  $\gamma = 2\pi \cdot r \cdot n / t$ , where  $r$ ,  $n$  and  $t$  are the distance from the torsion axes, the number of applied revolutions and the mean thickness of the sample, respectively.

To study the influence of the deformation temperature, Armco iron and P800 were subjected to warm and cold HPT. In the case of warm HPT, the deformation process was performed in the same tool by placing the two anvils and the sample into the inductor of an induction heating system. For cold HPT the anvils and the sample were placed into a cup that was then flushed with liquid nitrogen. With these tool supplements the sample can be deformed in a temperature range between 77 K and 873 K. Moreover, the tool allows variations in the applied strain, pressure and rotation speed and enables the direct measurement of the torque applied to the sample. Figure 1 shows a sketch of the used warm and cold HPT setup.

### 2.2 Microstructural investigations

To investigate the evolving microstructures, the samples were cut at a radius of 3 mm and examined in radial

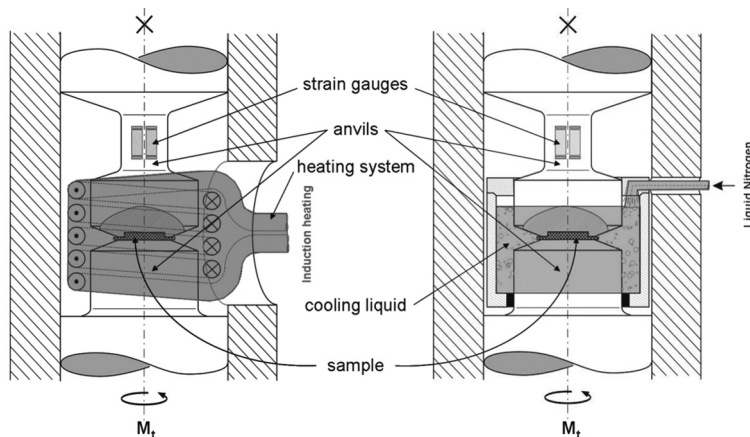


Fig. 1: Schematic illustration of the used HPT equipment for hot and cold processing

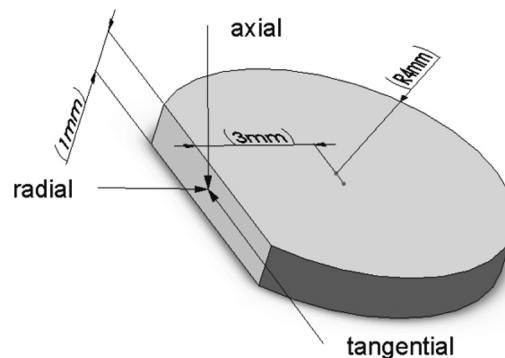


Fig. 2: Dimensions and definition of the sample directions for microstructural investigations

direction as depicted in Figure 2. The microstructural studies were performed within a LEO 1525 scanning electron microscope (SEM) by capturing secondary electrons (SE) and back scattered electrons (BSE) images. The energy and intensity of BSE depends, among the elements, the topography etc., on the orientation of the crystallites with respect to the direction of the incident electron beam. Thus, the captured images depict the grain and subgrain morphology of the SPD microstructures. For very small structural elements like in the ferritic steel the samples were studied inside a Philips CM12 transmission electron microscope (TEM). The grain size and other microstructural parameters were determined by the software analySIS from Soft Imaging Systems.

## 3. Results

### 3.1 Armco Fe

A sequence of BSE images is given in Figure 3a–3c, all taken at the same SEM magnification in radial direction at a radius of 3 mm showing the substructure in more detail. It provides an overview of the microstructure in the saturation obtained at different deformation conditions. The micrographs correspond to HPT deformation temperatures of 293 K, 543 K, and 723 K, respectively, at a strain rate of  $2.5 \times 10^{-3} \text{ s}^{-1}$ . The most conspicuous feature of the microstructure is that the size of the structural elements increases from about 150 nm to 450 nm after HPT at 293 K and 723 K, respectively. The microstructure after processing at 293 K is characterized by

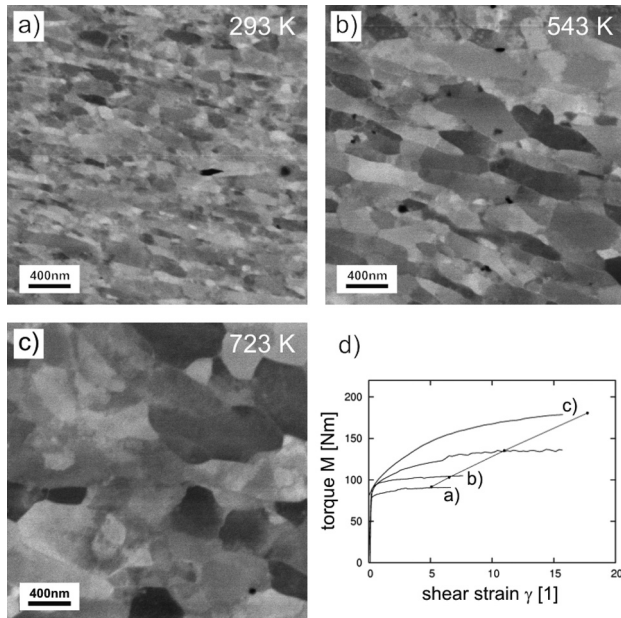


Fig. 3: Sequence of BSE images in the steady state regime taken in radial direction at a) 293 K, b) 543 K and c) 723 K; d) torque curves for various deformation conditions. The beginning of saturation is indicated by black dots

a large fraction of smeared boundaries between neighbouring structural elements. As the deformation temperature has increased, the boundaries become more clearly visible and the shape of the structural element is more polygonal.

The significant effect of deformation temperature on the structural size is reflected in the torque curves and depicted in Figure 3d. The total torque  $M$  vs. shear strain  $\gamma$  of various samples measured in situ during SPD at different temperatures, show all the same behaviour: a steep rise of the torque at low shear strains that decreases slightly with preceding deformation until a specific  $\gamma_s$  and  $M_s$  is reached. From the beginning of saturation (black dots in the diagram) the torque remains constant for all samples. It is clearly evident that the processing temperature essentially dominates both the saturation torque  $M_s$  and the saturation shear strain  $\gamma_s$ . An increase in the deformation temperature leads to a decrease in these two parameters. The onset of steady state is shifted towards lower torques and shear strains, respectively.

### 3.2 Ferritic steel P800

A collection of BSE micrographs obtained at an equivalent strain of  $\epsilon_{VM} \sim 32$  during warm and cold HPT is given in Figure 4. The samples were deformed in a temperature range between 77 K and 723 K. The BSE images clearly show that not only the size of the crystallites but also the sharpness of the boundaries has increased with increasing temperature. The pronounced polygonal grain shape and the uniform size distribution seem to be a characteristic feature for warm HPT. The mean size of the crystallites is about 120 nm and 270 nm after HPT at 293 K and 723 K, respectively.

Processing the same material at liquid nitrogen temperature, the microstructure can be refined to a mean structural size of about 40 to 80 nm. Due to these fine grains, the microstructure of low temperature samples

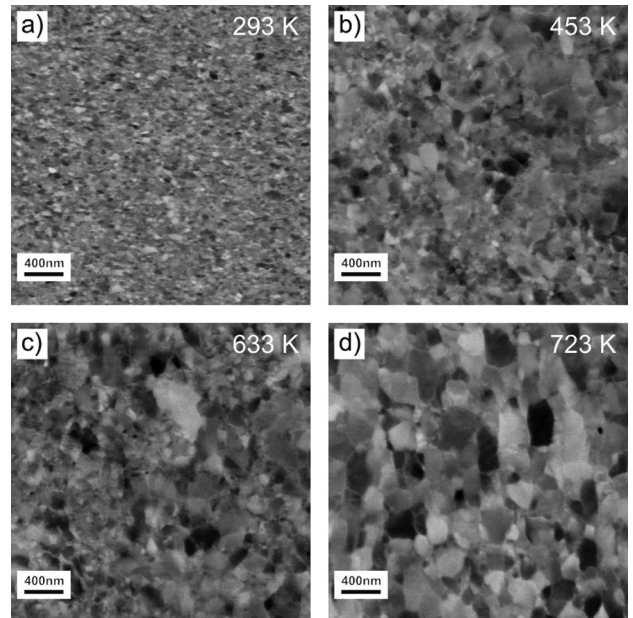


Fig. 4: BSE images of HPT deformed P800 in radial direction; the samples were deformed at different temperatures (see insets)

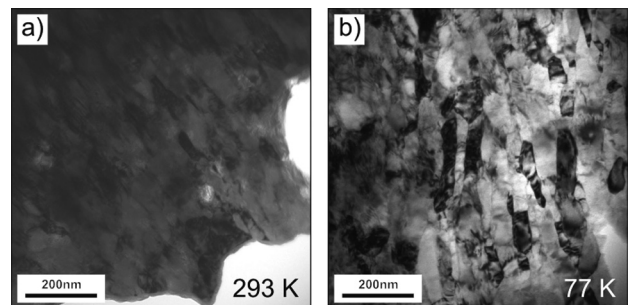


Fig. 5: TEM micrographs of P800 deformed at low temperatures (293 K and 77 K)

was analysed within a TEM. The images in Fig. 5 clearly show that the grains are mostly elongated parallel to the shear direction, especially at 77 K.

The above mentioned structural differences of Armco iron and P800 processed at various temperatures can be attributed to the different alloying components and, moreover, to a thermally induced decreasing dynamic recovery rate and dynamic restoration process similar to dynamic recrystallization. Figure 6 summarizes the observed mean structural size at saturation as a function of the processing temperature.

### 3.3 Pearlitic rail steel S900A

A sequence of SE and BSE images captured in tangential direction of the HPT deformed S900A is given in Figure 7a through c; the torque curves are given in Fig. 7d. The most apparent features of the deformed pearlitic steel are the fragmentation and the alignment of the cementite lamellae. At a small strain level in the range up to  $\epsilon = 4$  the cementite lamellae are heavily bent and partly broken, but the cementite colonies are still clearly visible (Figure 7a). Favourably oriented lamellae begin to align parallel to the shear plane. At higher strains (Fig. 7b and 7c) the lamellae are almost parallel aligned and some are broken into pieces smaller than

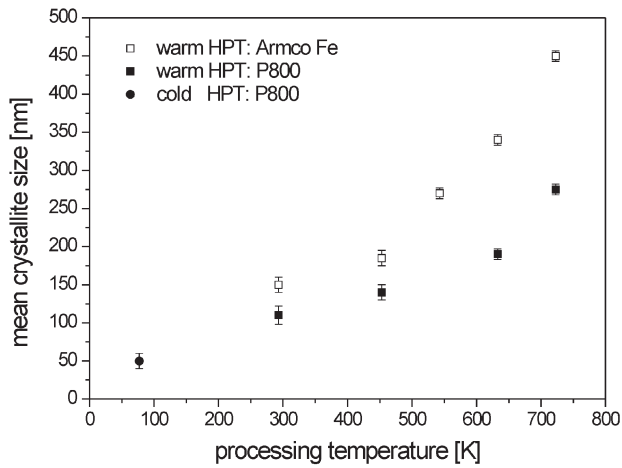


Fig. 6: Mean crystallite size for Armco iron and P800 at saturation as a function of processing temperature

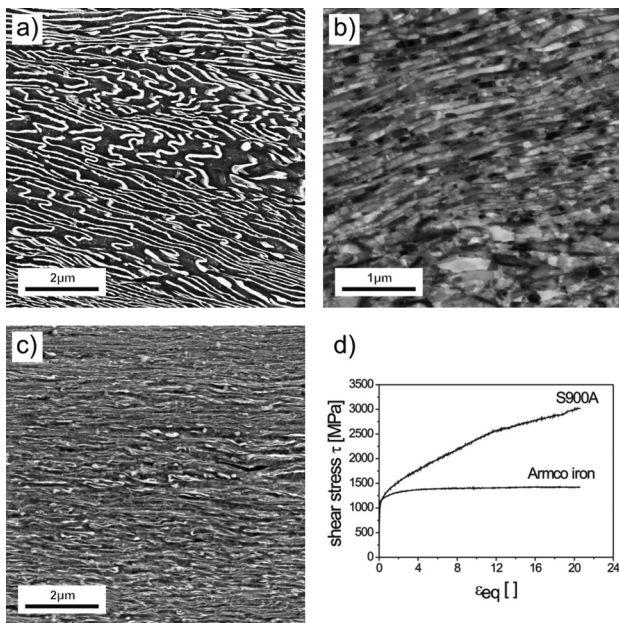


Fig. 7: SEM images of HPT deformed S900A in radial direction a)  $\epsilon=4$ , SE etched, b)  $\epsilon=8$ , BSE contrast, c)  $\epsilon=16$ , SE etched, d) torque curves

1  $\mu\text{m}$ . A nearly linear decrease of lamellae spacing with increasing strain can be observed.

The evolution of microhardness and the changes in structural size for Armco iron and S900A are summarized in Figure 8. When following the structural evolution of the ferrite phase one can observe in principle a similar behaviour as in Armco iron. Only the size of the structural elements is significantly smaller and no saturation is observed.

#### 4. Discussion

The investigated materials Armco iron and P800 showed that the shear flow stress approaches saturation at large strains, independent of applied deformation conditions. By comparing the torque curves one can clearly see that no decrease of the shear flow stress is observed even if the strain is larger than the shear strain  $\gamma_s$  at the onset of saturation. Thus, a process similar to the geometric

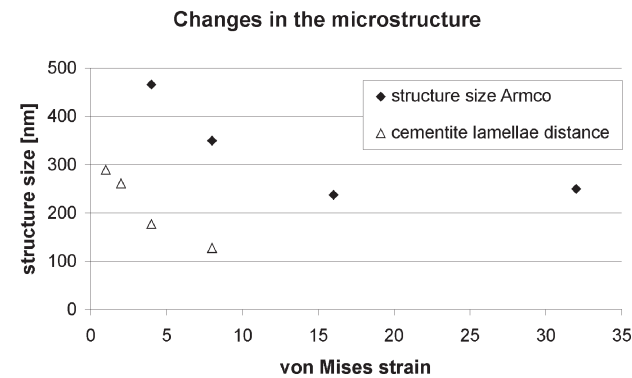
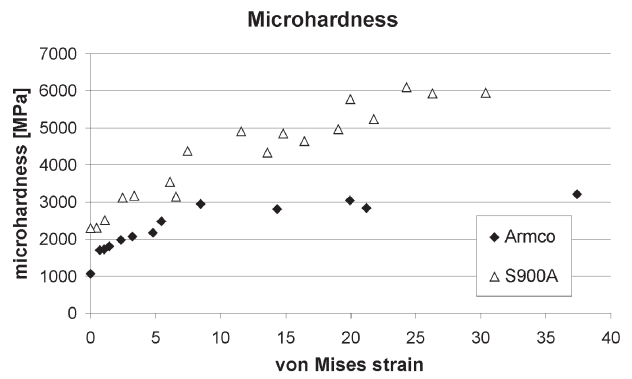


Fig. 8: Microhardness and microstructural size as a function of applied strain

dynamic recrystallization (GDRX)<sup>8</sup> rather than discontinuous dynamic recrystallization (DDRDX)<sup>9</sup> seems to be responsible for the existence of saturation at high temperatures. DDRX is understood as a two-stage process existing of the nucleation and growth of recrystallized grains resulting in a significant bimodality of microstructural sizes. GDRX is characterized by a small range migration of high angle dislocation boundaries towards opposite boundaries. During deformation the grains are significantly flattened until each side of the boundaries is separated by only a small distance. The structural elements are too small to generate new dislocation structures in their interior.

With decreasing temperature the thermal activation of dislocation processes and boundary mobility is reduced resulting in smaller grain sizes at 77 K. Dynamic recovery (DRV) and dynamic recrystallization (DRX) are inhibited at low temperatures and it seems that both play a minor role in the deformation process. The larger defect density remaining in the microstructure is stored in smaller structural elements which results in a higher shear stress at saturation. The reduced thermal activity and mobility of microstructural boundaries at low temperatures inhibit the dynamic formation of equiaxed structural elements. This is reflected especially in the elongated grain structure of the HPT deformed ferritic steel at low temperatures.

By comparing the ferritic steel with the pearlitic rail steel one can obtain in both materials structural elements of a size between 15 and 150 nm aligned parallel to the shear direction. In the case of P800 the mentioned restoration processes are responsible for the steady state microstructure. In the case of the pearlitic steel the sandwich structure existing of alternating "cementite" and ferrite phases, the restoration processes are inhibited.

ited which leads to a very fine grained deformation state. Without saturation in microstructural refinement a high stress is necessary for dislocations to cross a cementite lamellae and to deform the small grains. Hence, the lamellae will act as a barrier for the dislocations and they pile up at the interface if the stress is not high enough. The cementite lamellae are severely bent, at a certain stress they break and align parallel to favourable orientations. When the fragments are small enough they will be moved in the soft matrix without much further deformation. However, they hinder the movement of boundaries in the ferrite. When the local dislocation density is high enough carbon atoms are dragged into the ferrite matrix leading to an additional increase of hardness due to the solid solution hardening<sup>10,11</sup>. The sum of these effects causes the pronounced increase in strength without the development of saturation in the microstructural refinement and flow stress.

## 5. Conclusion

Armco iron, a ferritic steel P800 and a pearlitic rail steel S900A were subjected to SPD under various deformation conditions. Single phase and multi phase materials showed a different deformation behaviour. The most important characteristics that were observed during SPD can be summarized as follows.

1. With increasing SPD temperature the size of the structural elements in the steady state increases for Armco iron and P800. The differences in the element size at saturation can be attributed to reduced boundary mobility due to alloying.

2. The decrease in SPD temperature results in both the increase in strength and decrease in grain size. At low temperatures the microstructure of P800 exhibits remarkably elongated grains.

3. GDRX seems to be the governing restoration processes at high temperatures. The absence of DRV and DRX at low temperatures results in very fine grained micro/nanostructures in single phase materials.

4. The evolution of the microstructure and the mechanical strength in pearlitic rail steels is governed by three processes: the decreasing lamellae spacing, the increasing dislocation densities and the solution of carbon atoms in the ferrite matrix.

## 6. Acknowledgement

The financial support by the Christian Doppler Forschungsgesellschaft and the providing of testing material by Böhler Edelstahl GmbH is gratefully acknowledged.

## References

- <sup>1</sup> Vorhauer, A., T. Hebesberger, and R. Pippa: Disorientations as a function of distance: a new procedure to analyze local orientation data. *Acta Mater.* 51 (2003), 677–686. – <sup>2</sup> Hebesberger, T., H.P. Stüwe, A. Vorhauer, F. Wetscher, and R. Pippa: Structure of copper deformed by high pressure torsion. *Acta Mater.* 53 (2005), 393–402. – <sup>3</sup> A. Vorhauer, and R. Pippa: On the homogeneity of deformation by high pressure torsion. *Scripta Mater.* 51 (2004), 921–925. – <sup>4</sup> Wetscher, F., B. Tian; R. Stock, and R. Pippa: High pressure torsion of rail steels. *Mater. Sci. Forum* (2006), 455–460. – <sup>5</sup> Valiev, R. Z., R. K. Islamgaliev, and I. V. Alexandrov: Bulk nanostructured materials from severe plastic deformation. *Prog. Mater. Sci.* 45 (2000), 103–189. – <sup>6</sup> Scheriau, S., and R. Pippa: Influence of grain size on orientation changes during plastic deformation. *Mater. Sci. Eng., A* (2008). – <sup>7</sup> Pippa, R., F. Wetscher, M. Hafok, A. Vorhauer, and I. Sabirov: The limits of refinement by severe plastic deformation. *Adv. Eng. Mater.* 8 (2006), 1046–1056. – <sup>8</sup> McQueen, H.J., J.K. Solberg, and N. Ryum: Influence of ultra-high strains at elevated temperatures on the microstructure of aluminium. Part I. *Phil. Mag. A* (1989), 447–471. – <sup>9</sup> McQueen, H.J., and E. Ebangelista: Substructures in aluminium from dynamic and static recovery. *Czech. J. Phys.* (1988), 359–372. – <sup>10</sup> Danoix, F., D. Julien, X. Sauvage, and J. Copreaux: Direct evidence of cementite dissolution in drawn pearlitic steels observed by tomographic atom probe. *Mater. Sci. Eng., A* 250 (1998), 8–13. – <sup>11</sup> Languillaume, J., G. Kapelski, and B. Baudalet: Evolution of the tensile strength in heavily cold drawn and annealed pearlitic steel wires. *Mater. Lett.* 33 (1997), 241–245.